Available online at www.sciencedirect.com
SCIENCE DIRECT®
Journal of Nuclear Materials 350 (2006) 173–181
journal of nuclear materials
www.elsevier.com/locate/jnucmat

Analysis of WWER-440 and PWR RPV welds surveillance data to compare irradiation damage evolution

L. Debarberis [a], B. Acosta [a,*], A. Zeman [a], F. Sevini [a], A. Ballesteros [b], A. Kryukov [c], F. Gillemot [d], M. Brumovsky [e]

[a] *Joint Research Centre of the European Commission, Institute for Energy, P.O. Box 2, 1755 ZG Petten, The Netherlands*
[b] *Tecnatom, Avd. Montes de Oca 1, San Sebasitan de los Reyes, E-28709 Madrid, Spain*
[c] *Russian Research Centre Kurchatov Institute, Kurchatov Square 1, 123182 Moscow, Russia*
[d] *AEKI Atomic Research Institute, Konkoly Thege M. út 29-33, 1121 Budapest, Hungary*
[e] *NRI, Nuclear Research Institute, Husinec-Rez 130, 25068 Rez, Czech Republic*

Received 20 August 2005; accepted 9 January 2006

Abstract

It is known that for Russian-type and Western water reactor pressure vessel steels there is a similar degradation in mechanical properties during equivalent neutron irradiation. Available surveillance results from WWER and PWR vessels are used in this article to compare irradiation damage evolution for the different reactor pressure vessel welds. The analysis is done through the semi-mechanistic model for radiation embrittlement developed by JRC-IE. Consistency analysis with BWR vessel materials and model alloys has also been performed within this study. Globally the two families of studied materials follow similar trends regarding the evolution of irradiation damage. Moreover in the high fluence range typical of operation of WWER the radiation stability of these vessels is greater than the foreseen one for PWR.

1. Introduction

The reactor pressure vessel (RPV) is practically and economically irreplaceable; it has to operate for the whole life of the plant and is subjected to significant usage, ageing and degradation of the mechanical properties due to neutron irradiation.

Both WWER (water water energy reactor) and PWR/BWR (pressurised/boiling water reactor) pressure vessels are made of welded ferritic steel sections. The Russian designed WWER-440 employed Cr–Mo–V steels (i.e., 15Kh2MFa, 15Kh2NMFAA) while western PWR/BWR selected Mn–Mo–Ni type of steels (as 16MND5, A302 B, A508 cl. 2 and cl.3, A533 gr.B).

The WWER-440 RPVs are made only from welded forgings, i.e., from cylindrical rings and from plates forged into domes, so there are no axial welds. Typical welding material for WWER comes from submerged arc weld using Sv-10khMFTU or Sv-15khMFTU wire [1]. The cylindrical portion of a PWR RPV may have longitudinal (axial) welds in addition to circumferential welds if the vessel is

* Corresponding author. Tel.: +31 224 565130; fax: +31 224 565636.
E-mail addresses: luigi.debarberis@cec.eu.int (L. Debarberis), beatriz.acosta-iborra@jrc.nl (B. Acosta).

0022-3115/$ - see front matter © 2006 Elsevier B.V. All rights reserved.
doi:10.1016/j.jnucmat.2006.01.003

made from plates. The PWR's commonest welding technique is, as for WWERs, automated submerged arc using tandem weld wires of the required composition where the protective environment is provided by a granular flux. After welding a stress relief and tempering treatments are performed [2].

Both RPV types, and their respective welds in particular, are sensitive to radiation, which induces embrittlement of the material and is one of the life limiting factors of the component. The most important effect of the radiation damage is the increase in the ductile-to-brittle transition temperature (DBTT). RPV embrittlement is therefore monitored by means of surveillance programmes, which are important elements with high impact on the plant lifetime management [3]. Generally surveillance capsules containing specimens representative of the vessel beltline materials are placed at particular locations inside the vessel where they experience accelerated exposure. These capsules are withdrawn at regular intervals and the testing of their specimens make it possible to predict the vessel material properties degradation, provided the capsule irradiation conditions are representative of the vessel irradiation condition in terms of temperature, neutron field parameters, etc. Adequate and representative material sampling is also important; in this sense WWER and PWR approaches differ somewhat. For example WWER's sampling location ranges from the 1/4 thickness to the deep 3/4 thickness, whereas for PWRs base and heat affected zone samples are taken near the 1/4 thickness depth plane and weld sampling is done through the thickness with the exception of location within 12.7 mm from the root (or surface) of the weld. Another difference can be found in the chosen orientation of the specimens that for weld metal it is taken transverse to the weld (axial to vessel) for WWERs and following ASTM E-185 (both axial and transverse to vessel) for PWRs.

The above-mentioned differences can be, however, considered minor in determining the effect of neutron irradiation with the actual given uncertainties. It still remains rather complex to properly compare the stability of WWER-440 and PWR RPV welds to radiation embrittlement; in particular using the available surveillance data. The first difficulty arises from the fact that WWER-440 reactors operate at a temperature of 260–265 °C while PWR operate in general at 290–295 °C. The surveillance samples might even be at slightly higher temperatures due to possible overheating of the surveillance capsules; in particular at high gamma radiation rates and accelerated locations [4].

A second difficulty is due to the fact that the considered damage indexations are different; in Russian designed WWER-440 the typical neutron index that best correlate damage is defined to be the fluence of neutrons with energy above 0.5 MeV while in PWR the 1 MeV energy threshold for fast neutrons is used. Furthermore the neutron spectra and the fluence ranges are different, for example the WWER-440 materials are exposed to higher accumulated fluences. The fluence rate is also different for PWR and WWER-440, higher in general for the latter. Anyhow, fluence rate is not expected to play any role for matrix damage, whereas it might only affect precipitation and segregation in the low fluence range before appearance of saturation.

The third difficulty at the time of comparing both RPV types comes from their chemical composition mainly due to the different ranges of content in alloy, residual elements and related uncertainties.

In this study the comparison is made using available data from the open literature, mostly assembled in the frame of the AMES (Ageing Materials European Strategy) European Network [5]. In addition data recently elaborated by the authors and data from the model alloys programme of the JRC Institute for Energy are used in order to verify the differences and similitude of the different types of materials. The aim is to determine the different evolution of the irradiation damage in terms of the ductile to brittle transition temperature change using the semi-mechanistic model under development at the JRC Institute for Energy.

2. Damage mechanisms and their description

The present analysis is done based on the consideration of three basic mechanisms contributing to primary radiation embrittlement of steels and welds: direct matrix damage, irradiation induced precipitation and elements segregation.

Direct matrix damage is known to be the damage of the material due to basic defects formation; accounting for the observed damage in very clean (low copper and phosphorus) materials. For irradiation induced precipitation it is meant, in agreement with current knowledge, the damage due to the formation of copper nano-precipitates (other impurities might as well contribute but they are not considered here). It must be noted that there might be a link between direct matrix damage rate and the

copper nano-precipitates formation, in particular through the dependence of copper diffusivity. As regards to the accumulated damage, due to the different time scales involved anyhow, the matrix term and the copper precipitation term can be additively considered.

Elements segregation it is considered here as the phosphorus segregation at internal grain interfaces (dislocation planes, etc.) as observed in several atom probe works. Again nano-features seem responsible for mechanical properties deterioration is similar way to copper nano-precipitates.

Even thought that WWER-440 and PWR materials differ in chemical composition the underlying embrittlement mechanisms are the same, as it is confirmed by experimental studies, due to the common basic ferritic structure and the similar forming of copper and phosphorus nano-features in both types of RPV steels and welds.

The semi-mechanistic model to determine the ductile-to-brittle transition temperature shift, developed and tested recently by the JRC-IE, is used in this work [6]. In the model matrix damage contribution is generally assumed to have a square root dependence on fluence while precipitations and segregations of copper and phosphorus are considered to be saturation-type functions of fluence. Summarising, based on these three partial contributions, the total effect in term of $\mathrm{DBTT}_{\mathrm{shift}}$ is:

$$\mathrm{DBTT}_{\mathrm{shift}} = a \cdot \Phi^{0.5} + b \cdot \left[1 - \mathrm{e}^{-\Phi/\Phi_{\mathrm{sat}}}\right] + \frac{c}{2} \cdot \left[1 + \tanh\left(\frac{\Phi - \Phi_{\mathrm{start}}}{d}\right) - c_0\right], \quad (1)$$

where $\mathrm{DBTT}_{\mathrm{shift}}$ is the calculated transition temperature shift, Φ is the neutron fluence (10^{18} n cm^{-2}), a is a model fitting parameter for matrix damage, b is a model fitting parameter representing the maximum saturation value of the shift due to precipitations, Φ_{sat} is a model fitting parameter describing the start of saturation in the precipitation effect (the fluence at which 66% of b is reached), c is a model fitting parameter representing the saturation value of the shift due to segregation, Φ_{start} is a model parameter representing the fluence at which segregation starts, d is a model parameter representing the velocity of rising of $\mathrm{DBTT}_{\mathrm{shift}}$ due to segregation until the saturation value is reached and c_0 is the balance term to force the function to be exactly zero at zero fluence. The term c_0 is normally very small, responsible of a few °C offset, and it can be actually neglected.

Six parameters are required in total for the proposed model: a, b, Φ_{sat}, c, Φ_{start}, and d. The most important are a, b, and c. In most cases parameter b depends mainly on the Cu content and c on the P content ($b = b_1 \cdot (\mathrm{Cu}\text{-}0.05)$; $c = c_1 \cdot \mathrm{P}$, Cu and P are concentrations in mass%). The parameters Φ_{sat} and Φ_{start}, considered as 'time-dependent', model the influence of the fluence rate at which irradiation takes place [7].

3. Available data for this study

A number of data from the US and from the French surveillance programmes were compiled in 1996 by P. Petrequin in the AMES Report No. 6, EUR 16455 EN [8]. For this analysis welds data have been selected since experience has shown that the influence of irradiation on the welds is often greater than on the base material and welds are considered as one of the critical areas for plant life management. The US data set consists on 11 different RPV welds as summarised in Table 1. In order not to trace any particular reactor vessel the data are provided with identification codes.

As can be seen copper is varying widely from 0.04 to 0.28 mass%. Phosphorus ranges between 0.012 and 0.023 mass%; while nickel content is rather even and anyhow below 1 mass% which is normally considered threshold value for any significant Ni-effect [9].

The data set of French welds is then summarised in Table 2. Copper is varying in a narrower range when compared to the US set: between 0.03 and 0.13 mass%, whereas phosphorus content is in the range between 0.003 and 0.019 mass%. The content of nickel is always below the Ni-effect threshold.

Recently re-evaluated surveillance data from the Spanish PWR have become also available; a detailed description of the current status of the Spanish surveillance programme is given in [10]. This information constitutes a reasonable sample of data for the scope of this work and is certainly representative of PWR materials in general. For the Spanish welds the contents of copper (from 0.02 to 0.05 mass%) and phosphorus (from 0.004 to 0.01 mass%) are in the same range of the above-mentioned materials. The accumulated fluence for these welds ranges from 4.65×10^{18} n cm^{-2} to 5.5×10^{19} n cm^{-2} ($E > 1$ MeV).

The correlation matrix of copper and phosphorus contents for the available sets of PWR materials is given in Fig. 1. Such a plot shows that for the

Table 1
Summary of the US data on welds

ID	Cu (mass%)	P (mass%)	Ni (mass%)	Neutron fluences 10^{19} n cm^{-2} ($E > 1$ MeV)	$DBTT_{shifts}$ (°C)
WA	0.230	0.012	0.56	0.7–1.01–1.75	78–92–83
WB	0.050	0.013	0.91	0.64–1.47	17–42
WC	0.040	0.015	0.67	0.38	0
WD	0.066	0.015	0.71	0.31	33
WE	0.130	0.017	0.09	0.55–1.25–4	18–32–72
WF	0.190	0.017	0.15	1.2–5.1	44–81
WG	0.280	0.017	0.71	0.28–0.57	86–106
WH	0.180	0.019	0.57	0.54–2.1	61–92
WI	0.086	0.020	0.11	0.25–0.83	43–42
WJ	0.270	0.023	0.74	0.18–0.62–1.06–1.88	44–92–111–114
WK	0.055	0.022	0.97	0.85	39

Table 2
Summary of the French data on welds

ID	Cu (mass%)	P (mass%)	Ni (mass%)	Neutron fluence 10^{19} n cm^{-2} ($E > 1$ MeV)	$DBTT_{shifts}$ (°C)
WA	0.030	0.003	0.78	1.38–2.23	18–26
WB	0.030	0.004	0.78	0.92	14
WC	0.040	0.004	0.60	1.39	8
WD	0.030	0.005	0.52	1.32	0
WE	0.030	0.005	0.77	1.65	22
WF	0.030	0.005	0.61	0.85	1
WG	0.030	0.007	0.70	0.87	26
WH	0.040	0.007	0.75	1.17–2.40	18–22
WI	0.030	0.008	0.73	1.15–1.57–2.73	31–31–37
WJ	0.030	0.008	0.71	1.26–2.50	41–45
WK	0.031	0.008	0.66	1.78–3.70–5.19	24–42–57
WL	0.030	0.008	0.70	1.28–1.36	34–44
WM	0.030	0.008	0.70	2.59–3.90	48–72
WN	0.033	0.008	0.64	1.19–2.78–3.62	10–26–25
WO	0.030	0.009	0.70	1.29	38
WP	0.070	0.009	0.64	1.26–2.52	29–43
WQ	0.030	0.009	0.64	1.50–2.36–3.33	19–35–42
WR	0.030	0.009	0.66	1.25–2.55–3.46	12–28–29
WS	0.030	0.009	0.72	1.35–3.25–4.22	15–31–32
WT	0.030	0.009	0.66	1.79–3.58–5.58	26–30–45
WU	0.030	0.010	0.68	1.33–2.56	23–38
WV	0.120	0.012	0.07	0.31–2.25	8–38
WW	0.041	0.013	0.57	1.29–2.76	38–51
WX	0.040	0.013	0.57	1.24–2.49	31–30
WY	0.110	0.014	0.58	0.60	33
WZ	0.040	0.014	0.55	1.83–3.69–4.85	33–45–51
WAA	0.040	0.014	0.55	1.28–2.60–3.54	38–53–72
WBB	0.040	0.015	0.56	1.86–4.06–5.81	20–42–61
WCC	0.100	0.015	0.51	0.33–1.53–2.38	11–63–44
WDD	0.100	0.016	0.49	0.47–2.20	27–63
WEE	0.090	0.017	0.10	0.36–2.34	21–37
WFF	0.130	0.017	0.08	0.34–2.16	15–35
WGG	0.100	0.019	0.09	0.32–2.26	12–36

studied PWR welds there is no preferential correlation between Cu and P, therefore for modelling purposes the parameters b_1 and c_1 of Eq. (1) can be considered independent from each other.

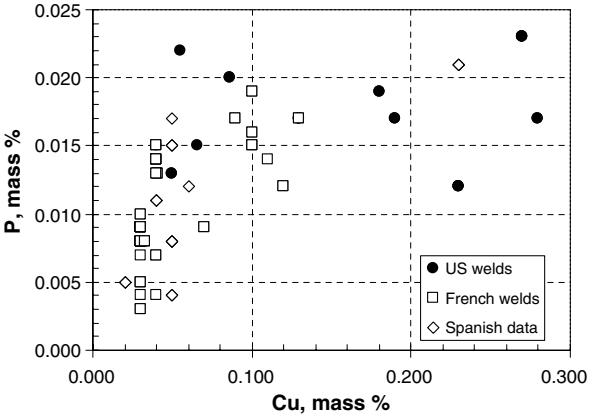

Fig. 1. Copper and phosphorus content matrix for PWR data.

The WWER-440 weld data [11] considered here are those already studied in a previously published work [12]. Main features of this data are that, similarly to the PWR data, copper is varying between 0.06 and 0.24 mass%, while phosphorus content is higher than for PWR welds, ranging from 0.01 up to 0.053 mass% and a certain degree of correlation between copper and phosphorus contents is found, see Fig. 2.

Although that damage indexation for WWERs is considered for neutrons with $E > 0.5$ MeV, accumulated fluences for WWER reactors are higher than those for PWR; in our case ranging from 8×10^{18} n cm^{-2} to 5.7×10^{20} n cm^{-2} ($E > 0.5$ MeV).

Other sets of data relative to BWR and model alloys are used for verification and discussion. BWR data are available from the NRC web site [13]. For this work data sets in the copper range

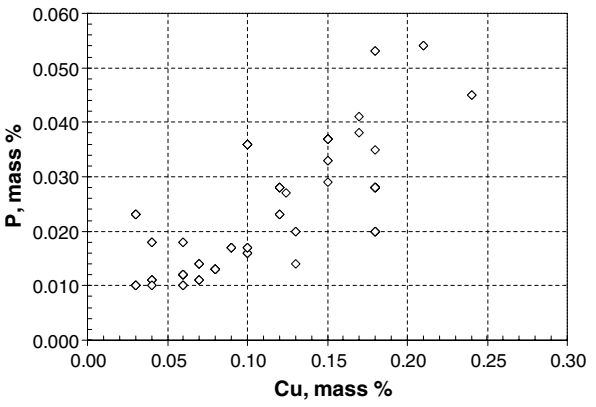

Fig. 2. Copper and phosphorus content matrix for WWER-440 welds.

Table 3
Summary of the selected model alloys data

ID	Cu (mass%)	Ni (mass%)	P (mass%)	Neutron fluence 10^{19} n cm^{-2} ($E > 0.5$ MeV)	$DBTT_{shifts}$ (°C)
637	0.10	0.006	0.012	0.75–6.5	30–46
639	0.40	0.004	0.002	6.5	87
640	0.41	0.004	0.012	0.75–6.5	115–119
175	0.11	1.140	0.010	0.75–6.5	120–223

between 0.1 and 0.2 mass% have been selected. In total 55 data points with fluences ranging from 2×10^8 n cm^{-2} up to 1.14×10^{11} n cm^{-2} ($E >$ 1 MeV).

To complete the study a selection of model alloys is also added to the analysis. The model alloys have been used by the JRC-IE to study the embrittlement mechanisms, the role of alloying element and impurities on embrittlement and the effect of fluence rate on the response to irradiation [14–16]. The selected model alloys have a composition comparable to previously analysed PWR, WWER and BWR data; their characteristic are given in the Table 3. As it can be seen in Table 3 a model alloy with high nickel content is also included for comparison.

4. Results and discussion

In order to properly compare the different contributions to $DBTT_{shift}$ on PWR and WWER materials we must consider the different neutron fluence indexation. In fact the accumulated fluence of neutrons with energy $E > 0.5$ MeV is, slightly depending on local spectrum, much higher than that for neutrons with $E > 1$ MeV. Typically for surveillance positions in WWER-440 reactors [17]:

$$\frac{\Phi_{E>0.5\ \mathrm{MeV}}}{\Phi_{E>1\ \mathrm{MeV}}} = 1.75. \quad (2)$$

The contribution of matrix damage to $DBTT_{shift}$ is modelled by a square root dependence on the accumulated fluence and by the parameter a, see Eq. (1). The parameter a has been calculated using the data points that belong to welds with low contents of copper and phosphorus so that the major contribution to DBTT shift is due to matrix damage.

The obtained a values for PWR and WWER-440 are 5.5 and 6.8, respectively, which are in agreement with the findings of Fisher and Buswell [18]. In Fig. 3 the comparison between PWR and WWER matrix damage terms is shown. The accumulated

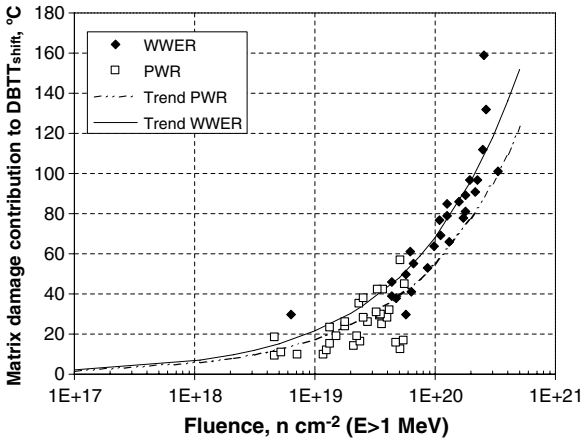

Fig. 3. Comparison of matrix damage contributions to $DBTT_{shift}$.

fluence for WWER-440 data has been adjusted according to Eq. (2).

The observed difference in the a parameter can be entirely attributed to the different operation temperatures of WWER (270 °C) and PWR (290 °C). In fact if a 'temperature factor' in the form of Eq. (3) is considered [19], the ratio between the parameters a for both WWER and PWR is ≈1.24.

$$TF_a(T) = \frac{F_a}{e^{\left(-\frac{E_a}{kT}\right)}} = 2.7 \times 10^{-3} \cdot e^{\frac{3.3\times10^3}{T}}. \quad (3)$$

According to this we can reproduce the different studied $DBTT_{shift}$ data using the semi-mechanistic model of Eq. (1), optimising the values of the parameters b_1 and c_1 and considering saturation fluences in the range of 10^{19} n · cm^{-2}, in agreement with previous studies [18]. The obtained parameters for PWR and WWER welds are shown in Table 4.

As can be seen in Fig. 4, satisfactory results, even considering the intrinsic scatter of the data ($\sigma \approx 25$ °C on WWER-440 welds), can be achieved.

As regards irradiation induced precipitation and elements segregation, mainly due to copper and phosphorus, respectively, their contribution to the $DBTT_{shift}$ is developing in different ways for WWER-440 and PWR welds. WWER-440 exhibits slightly higher values of the parameters b_1 and c_1 than PWR, in the range of 17%, which can be fully explained by the lower operational temperature of WWER reactors. In fact at higher irradiation temperatures the rate of damage is considered to be decreasing, due to increased mobility of atoms and

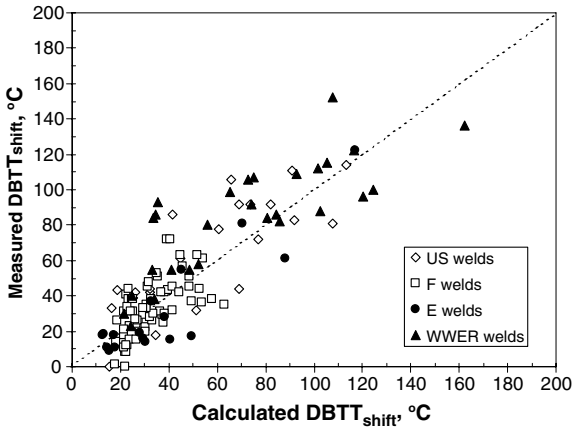

Fig. 4. Calculated versus measured $DBTT_{shifts}$ for the studied data.

Table 4
Summary of semi-mechanistic model parameters

Parameter	Modelling	PWR welds	WWER-440 welds	Difference	Remarks
a	Matrix damage rate	5.5	6.8	~20%	Higher in WWER due to lower operational temperature
b_1	Effect of copper at saturation	400	480	~17%	Slightly higher for WWER-440 due to the lower operational temperature
c_1	Effect of phosphorus at saturation	2500	3000	~17%	Idem
$\Phi_{sat}\times10^{18}$	Start of saturation of precipitation	8	55	~85%	Much higher for WWER-440 due to lower temperature and different material structure
$\Phi_{start}\times10^{18}$	Start of saturation of segregation	9	100	~91	Much higher for WWER-440 due to lower temperature and different material structure

enhanced recombination of the interstitials and vacancies created by the neutron irradiation as well as the diffusion of individual elements.

Conversely, differences are found in relation to the 'time-dependent' parameters of the model. In particular the fluences for saturation of precipitation and segregation effects appear to be higher for WWER-440. This is certainly caused by the lower operational temperature (since diffusion, segregation and other thermally activated processes are slowed down) but also by the different structure of the material (Cr–Mo–V) and the different content of other alloying elements like manganese. Regarding the different fluence rates for WWER and PWR, it should be noted that the data used for this study are outside the fluence range where flux can have a significant effect.

If we take into account the different fluence indexation for WWER-440, the two families of materials seem to follow similar trends for what regards the evolution of the $DBTT_{shift}$. The latter can be directly observed, for example, selecting the PWR and WWER-440 data with similar low phosphorus content and within a narrow range of copper (between 0.1 and 0.13 mass%) and plotting them together as in Fig. 5 (the fluence for WWER-440 is adjusted using Eq. (2).). However, if we consider also the temperature effect the radiation stability of WWER-440 welds appears to be, in the high fluence range, greater than the foreseen PWR trend.

It should be noted that any decrease effect after the 'Cu precipitation peak-hardening', observed for thermal ageing by Fujii et al. [20] and by Russell and Brown [21], possibly appearing at fluences higher than Φ_{sat}, could not be identified in the analysed dataset and therefore not considered neither in this study nor in the development of the semi-mechanistic model for $DBTT_{shift}$ and their parameters.

The operational temperature of the BWR is similar to that of WWER-440, so similar behaviours with respect to embrittlement are a-priori expected. In order to verify the consistency of the findings a set of BWR data, with similar Cu and P contents than the previously studied welds, is used. Moreover the JRC model alloys, irradiated at 270 °C for two accumulated fluences, are also included for confirmation.

We can check up again that, once the same neutron indexation is used, in Fig. 6 no big differences are observed amongst the various families of materials with low nickel content for what regards radiation stability.

The BWR selected data are in fact following the same global trend of WWER-440. The model alloys with low nickel are also in line with the other data considering that they have upper and lower extreme copper contents (0.1 mass% for MA 637 and 0.4 mass% for 639 and 640) in comparison with the other data.

The lower trend in Fig. 6 is provided by the $DBTT_{shift}$ semi-mechanistic model applying the average parameters observed on the studied welds.

The situation completely changes when we consider high nickel materials; for comparison one high nickel model alloy (MA 176, open dots in Fig. 6) has also been included in the study. The measured DBTT shifts are significantly higher than those observed for the other studied welds and therefore completely different $DBTT_{shift}$ trend is obtained.

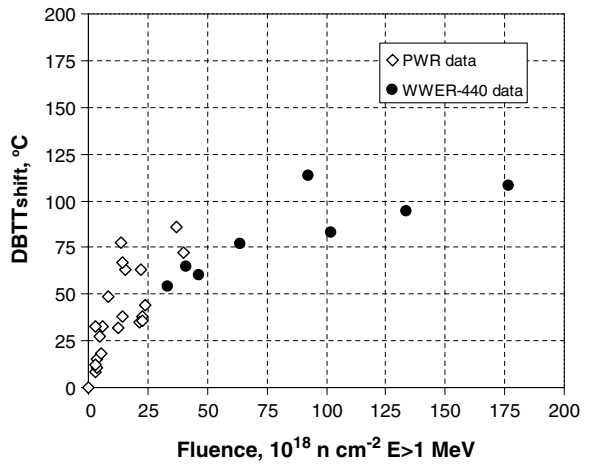

Fig. 5. $DBTT_{shifts}$ versus fluence; copper range data: 0.1–0.13 mass%.

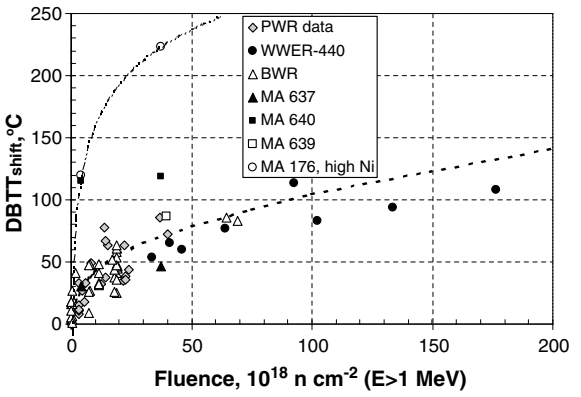

Fig. 6. Comparison of $DBTT_{shifts}$ for PWR, WWER and BWR welds and for model alloys.

This is in agreement with the previous findings on model alloys [16]: nickel increases the matrix damage rate and has an influence on the precipitation (synergism with copper [22]) and segregation parameters enhancing the contribution to $DBTT_{shift}$ of such effects.

5. Conclusions

WWER-440 and PWR RPV materials are subjected to significant radiation and in particular the welds need to be carefully monitored. The available results from surveillance data can be used, as it is done in this paper, to study and compare the behaviour of the different families of materials. Also data on BWR and model alloys can be used to verify the consistency of the findings.

In spite of the encountered difficulties to compare both PWR and WWER weld types some important conclusions can be drawn:

- Matrix damage rates are basically equal for both weld types, the observed differences can be attributed to the different operation temperatures of WWER and PWR. For modelling purposes unified temperature dependent matrix damage parameter can be used for the two families of materials.
- Precipitation and segregation coefficients are quite similar for the different welds, the apparent higher observed damage for the WWER-440 welds is, for the same phosphorus level, mainly due to the higher radiation level at which the materials are exposed and the slightly lower temperature at which they are operated.
- Fluences at which segregation and precipitation effects start to saturate are higher for WWER-440 than for PWR welds due to the lower operational temperature, the Cr–Mo–V structure of the material and the different content of other alloying elements.

Taking into account the different fluence indexation for WWER-440 the two families of materials follow similar trends for what regards the evolution of the irradiation damage. However, if we consider the temperature effect the radiation stability of WWER-440 is in the high fluence range greater than the one foreseen for PWR.

The obtained results are very promising and further work is required to single out the role of other elements, like nickel and manganese. Also the influence of other radiation field parameters, like neutron spectra, needs to be analysed in more details. A larger qualified database would also improve the accuracy of the parameters determination.

To cope with these open issues the JRC-IE is currently carrying out new experimental research through specially tailored model steels and realistic welds.

Acknowledgement

The authors would like to thank Dr W. Server for providing complementary data and suggestions for this work.

References

[1] Guidelines for prediction of irradiation embrittlement of operating WWER-440 reactor pressure vessel, IAEA-TEC-DOC-1442, IAEA, Vienna, 2005.
[2] L.M. Davies, A comparison of western and eastern nuclear reactor pressure vessel steels, AMES Report No. 10, EUR 17327, European Commission, Luxembourg, 1997.
[3] R. Gerard, Survey of national regulatory requirements, AMES Report No. 4, EUR 16305, European Commission, Luxembourg, 1995.
[4] A. Ballesteros, J. Bros, L. Debarberis, F. Sevini, D. Erak, S. Gezashchenko, A. Kryukov, Y. Shtrombakh, G. Goloschapov, Nucl. Eng. Des. 235 (2005) 411.
[5] F. Sevini, L. Debarberis, K. Törrönen, R. Gerard, L.M. Davies, Int. J. Pres. Ves. Pip. 81 (2004) 683.
[6] L. Debarberis, A. Kryukov, F. Gillemot, B. Acosta, F. Sevini, Int. J. Pres. Ves. Pip. 82 (2005) 195.
[7] L. Debarberis, B. Acosta, F. Sevini, A. Chernobaeva, A. Kryukov, J. Nucl. Mater., in press, doi:10.1016/j.jnucmat.2005.11.017.
[8] P. Petrequin. A review of formulas for predicting irradiation embrittlement of reactor vessel materials, AMES Report No. 6, EUR 16455, European Commission, Luxembourg, 1996.
[9] T.J. Williams, Int. J. Pres. Ves. Pip. 81 (2004) 657.
[10] A. Ballesteros, I. Marcelles, J. Bros, Nucl. Eng. Int. (2003) 32.
[11] N.N. Alekseenko, A. Amaev, I. Gorynin, V.A. Nikolaev, Radiation Damage of Nuclear Power Plant Pressure Vessel Steels, American Nuclear Society ANS, IL, 1997.
[12] L. Debarberis, B. Acosta, F. Sevini, A. Kryukov, D. Zhurko, in: Proceedings of IAEA International Conference on Irradiation Embrittlement, Gus, Russia, May 2004.
[13] NRC, Reactor Vessel Integrity Database Version 2.0.1, US, 2000.
[14] L. Debarberis, F. Sevini, B. Acosta, A. Kryukov, Y. Nikolaev, A.D. Amaev, M. Valo, Int. J. Pres. Ves. Pip. 79 (2002) 637.
[15] L. Debarberis, F. Sevini, B. Acosta, A. Kryukov, D. Erak, Int. J. Pres. Ves. Pip. 82 (2005) 373.

[16] L. Debarberis, B. Acosta, F. Sevini, A. Kryukov, F. Gillemot, M. Valo, A. Nikolaev, M. Brumovsky, J. Nucl. Mater. 336 (2005) 210.
[17] A. Ballesteros, Conversion table of material damage indexation for all different European reactor types. AMES Rep. 13, EUR 18693b, European Commission, Luxembourg, 1999.
[18] S.B. Fisher, J.T. Buswell, Int. J. Pres. Ves. Pip. 27 (1987) 91.
[19] L. Debarberis, B. Acosta, A. Zeman, F. Sevini, A. Ballesteros, A. Kryukov, F. Gillemot, M. Brumovsky, Scr. Mater. 53 (2005) 769.
[20] A. Fujii, M. Nemoto, H. Suto, K. Monma, Trans. JIM 9 (1968) 374.
[21] K. Russell, L.M. Brown, Acta Metall. 20 (1972) 969.
[22] G.R. Odette, Scr. Metall. 17 (1983) 1183.